Eur. Phys. J. B **29**, 147–152 (2002)
DOI: 10.1140/epjb/e2002-00273-y

THE EUROPEAN PHYSICAL JOURNAL B

Tunneling time in magnetic barrier structures

Feng Zhai[1,2,a], Yong Guo[1], and Bing-Lin Gu[1,2]

[1] Department of Physics, Tsinghua University, Beijing 100084, PR China
[2] Center for Advanced Study, Tsinghua University, Beijing 100084, PR China

Received 4 March 2002 / Received in final form 22 May 2002
Published online 17 September 2002 –

Abstract. We adopt the group velocity approach to the issue of tunneling time in two configurations of magnetic barrier structures, which are arranged with identical or unidentical building blocks. The effects of an external electric field are also taken into account. The tunneling time in magnetic barrier structures is found to be strongly dependent on the magnetic configuration, the applied bias, the incident energy as well as the longitudinal wave vector. The results indicate that for electrons with equal energy but different incident angles, the tunneling processes are significantly separated in time within the same magnetic barrier structure. In the configuration arranged with unidentical building blocks, there exists obvious asymmetry of tunneling time in two opposite tunneling directions. Such a discrepancy of the tunneling time varies distinctly with the longitudinal wave vector and the applied bias.

PACS. 73.40.Gk Tunneling – 75.75.+a Magnetic properties of nanostructures – 73.23.-b Electronic transport in mesoscopic systems

1 Introduction

Recently there has been an increasing interest in the transport properties of a two-dimensional electron gas (2DEG) subjected to perpendicular inhomogeneous magnetic fields on a nanometer scale [1–12]. Such magnetic fields can be patterned experimentally in the desired shape by means of deliberately shaping or curving the 2DEG [2], or covering the heterostructures with stripes of ferromagnetic or superconducting materials [3,4]. Theoretically, studies have indicated many intriguing phenomena caused by nonuniform magnetic fields, such as commensurability effects [5] and magnetic edge states [6]. Proposed and realized magnetic structures include magnetic dots, antidots, steps, wells, barriers, wires, rings, periodic and quasiperiodic superlattices. These quantum structures greatly extend the field of low dimensional quantum systems. Among them, the magnetic-barrier (MB) tunneling structure proposed by Matulis *et al.* [7], has been investigated widely [7–11] because of the novelty and potential applications as magnetic field sensors, magnetic memory elements, and nanomagnetometers [8]. The quantum transport through a MB structure is a 2D process in nature and possesses the wave vector filtering properties [7,8,11].

With the advance on miniaturizing tunneling semiconductor devices, the time aspect of tunneling process has been the focus of much research in the last decade. Apart from its intrinsic quantum mechanics interest, the significance of tunneling time comes from the requirement of understanding the tunneling dynamics in high-speed devices [13–29]. Therefore, even for a simple single-barrier structure, the tunneling time has been studied extensively by various theoretical approaches, such as phase-delay method [13], dwell time approach [14], Larmor Clock time and its generalizations [15], and wave packets evolvement method [16,17]. In double-barrier heterostructures, many effects on the tunneling time were examined, which include position-dependent effective mass [18], spin-orbit coupling [19], and structural asymmetry [20,21]. In a finite superlattice, the superlattice-tunneling-time limit was observed experimentally [22] and confirmed theoretically [23]. Recently, in semimagnetic semiconductor multilayers Guo *et al.* found obvious spin separation features in time [24]. Up to now, although there exists a great deal of published literature on the tunneling time, how to define a physical tunneling time is still the subject of much controversy. The reason is that time is not an operator in quantum mechanics [17]. The time characteristics introduced in the above-mentioned methods really describe different aspects of electron dynamics and can be extracted from corresponding optical or transport experiments.

How long does an electron tunnel through a magnetic-modulated quantum structure? This question is much of importance both from a theoretical and from a practical point of view. To the best of our knowledge, there is no work dealing with it. In the present paper, we explore characteristics of the tunneling time in MB structures, which consist of two identical (or unidentical) magnetic barriers and magnetic wells. The results indicated that

[a] e-mail: fzhai@castu.tsinghua.edu.cn

the tunneling time exhibits remarkable dependence on the longitudinal wave vector as well as the applied bias. In MB structures arranged with unidentical building blocks, the discrepancy of tunneling time between opposite tunneling directions is examined.

2 Method

The system considered here is a 2DEG in the presence of a perpendicular magnetic field (parallel to z direction) and an external electric field $\mathbf{F}$ (along the x direction). The magnetic field is homogeneous in the y direction and varies along the x axis. The MB quantum structure we investigate is composed of two building blocks A and B separated by a zero magnetic-filed region with width l, each of which includes one magnetic barrier with height B_i and width d_i, one magnetic well with depth $-B_i$ and width d_i (i=1, 2). The rectangular magnetic-field profile can be viewed as the limit of a small distance between the 2DEG and the ferromagnetic thin film [12].

Within the effective-mass approximation such a system is described by the Hamiltonian

$$H = \frac{1}{2m^*}(\mathbf{P} + e\mathbf{A}_i)^2 - \frac{eV_a x}{L}, \tag{1}$$

where m^* is the effective mass of the electron, $\mathbf{P}$ is the momentum operator, e is the proton's charge, $\mathbf{A}_i = (0, A_i(x), 0)$ is the vector potential given in the Landau gauge, and $V_a = FL$ ($L = 2d_1 + 2d_2 + l$) is the applied bias. Using the cyclotron frequency $\omega_c = eB_0/m^*$ and the magnetic length $l_B = \sqrt{\hbar/eB_0}$, we express all quantities in dimensionless units, for example, the coordinate $\mathbf{R} \to l_B\mathbf{R}$, the energy $E \to \hbar\omega_c E$, the time $\tau \to \omega_c^{-1}\tau$. Taking m^*= 0.067 m_0 (m_0 is the free electron mass) for the GaAs 2DEG and an estimated magnetic field $B_0 = 0.1$ T, we have $l_B = 813$ Å, $\hbar\omega_c = 0.17$ meV [7], and $\omega_c^{-1} = 3.81 \times 10^{-12}$ s. The total wave function can be written as $\Phi(x, y) = \mathrm{e}^{\mathrm{i}k_y y}\Psi(x)$, where $\Psi(x)$ satisfies the reduced one-dimensional Schrödinger equation

$$-\frac{1}{2}\frac{\mathrm{d}^2\Psi}{\mathrm{d}x^2} + U_{eff}(x, k_y, V_a)\Psi = E\Psi. \tag{2}$$

Note that the effective potential $U_{eff}(x, k_y, V_a) = \frac{1}{2}[k_y + A_i(x)]^2 - \frac{eV_a x}{L}$ depends on the longitudinal wave vector k_y, the applied bias V_a as well as the profile of the local magnetic field. In equation (1) we neglect the Zeeman term $g^*\mu_B B_i(x)\sigma_z/2$ [30], where g^* is the effective g-factor (in GaAs 2DEG $g^* = 0.44$), μ_B the Bohr magneton, $\sigma_z = +1/-1$ for electrons with up/down spin. The reason is that the absolute value of such a term is much smaller than that of other terms in U_{eff} (the ratio between them is about $g^*m^*/2m_0 = 0.015$).

We consider the situation that electrons tunnel through the MB structure from the left ($x < 0$) to the right ($x > L$). The wave functions in the left and right region can be written as $\Psi_L(x) = [\exp(\mathrm{i}k_L x) + r\exp(-\mathrm{i}k_L x)]/s$, $\Psi_R(x) = \exp(\mathrm{i}k_R x)$. Here, r, s are the reflection and transmission amplitudes, $k_L = \sqrt{2[E - U_{eff}(-\infty)]}$ and $k_R = \sqrt{2[E - U_{eff}(+\infty)]}$ are the wave vectors of incident (reflection) and transmission waves, respectively. In the present paper, we adopt the group velocity approach [25] to evaluate the tunneling time. From the semiclassical point of view, the group velocity $v_g(x)$ can be defined as the ratio between the averaged current probability density J [$J = \mathrm{Im}(\Psi^*\frac{d\Psi}{\mathrm{d}x})$, in units of $\frac{\hbar}{m^* l_B}$] and the probability density $|\Psi|^2$ of the particle. Note that J is conserved during the tunneling process and thus position-independent. As a result, we have $J = k_R$. Further, the tunneling time is

$$\tau = \int_0^L \mathrm{d}x/v_g(x) = \int_0^L \mathrm{d}x\,|\Psi|^2/J. \tag{3}$$

This intuitive definition, although apparently based on a semiclassical interpretation, has been shown to be equivalent to the Bohm tunneling time [17]. Numerical simulations on this definition indicated the agreement with experimental results [26].

Introducing five dimensionless variables $y_1 = \mathrm{Re}\Psi$, $y_2 = \mathrm{Im}\,\Psi$, $y_3 = (1/k_R)\mathrm{d}y_1/\mathrm{d}x$, $y_4 = (1/k_R)\mathrm{d}y_2/\mathrm{d}x$, $y_5 = \int_x^L \mathrm{d}x'(y_1^2 + y_2^2)$, one can obtain the following first-order ordinary differential equations (ODEs)

$$\begin{aligned}
&\frac{\mathrm{d}y_1}{\mathrm{d}x} = k_R\, y_3,\ \frac{\mathrm{d}y_3}{\mathrm{d}x} = 2(U_{eff} - E)\ y_1/k_R,\\
&\frac{\mathrm{d}y_2}{\mathrm{d}x} = k_R\, y_4,\ \frac{\mathrm{d}y_4}{\mathrm{d}x} = 2(U_{eff} - E)\ y_2/k_R,\\
&\frac{\mathrm{d}y_5}{\mathrm{d}x} = -\ (y_1^2 + y_2^2)
\end{aligned} \tag{4}$$

with initial value

$$(y_1, y_2, y_3, y_4, y_5)\ |_{x=L-} = (1, 0, 0, 1, 0). \tag{5}$$

We integrate the ODEs (4), (5) to get the vector (y_1, y_2, y_3, y_4, y_5)$|_{x=0+}$ by using of Gear's stiff method [31]. The tunneling time τ and transmission amplitude s (thus the transmission coefficient $\frac{k_R}{k_L}|s|^2$) can be evaluated by

$$\tau = y_5(0+)/k_R \tag{6}$$

and

$$s = 2/\left\{\left[(y_1(0+) + \frac{k_R}{k_L}y_4(0+)\right] + \mathrm{i}\left[y_2(0+) - \frac{k_R}{k_L}y_3(0+)\right]\right\}. \tag{7}$$

In deriving equations (5, 7), the continuity of wavefunction Ψ and its derivative $\frac{\mathrm{d}\Psi}{\mathrm{d}x}$ is used.

3 Results and discussion

We evaluate the tunneling time of a conduction electron traversing two different configurations of magnetic-modulated structures based on a GaAs 2DEG. One is

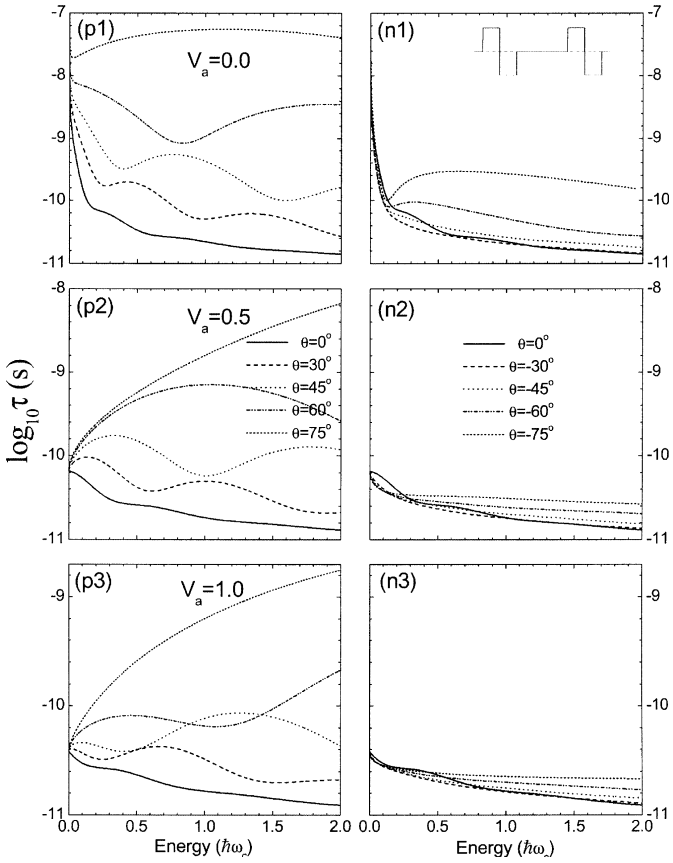

Fig. 1. The tunneling time for electrons traversing a "symmetric" MB structure at several incident angles under zero and two applied biases. The structure depicted in the inset of panel (n1) is composed of two identical blocks A ($B_1 = 0.1$ T and $d_1 = 1$) separated by a zero magnetic-field region with width $l = 3$. The left and right panels correspond to $\theta \geqslant 0$ and $\theta \leqslant 0$, respectively. $V_a = 0$, 0.5, 1.0.

an arrangement with two identical building blocks A, the other is composed of two different blocks A ($B_1 = 0.1$ T, $d_1 = 1$) and B ($B_2 = 0.3$ T, $d_2 = 1$). In both cases, there exists a zero magnetic-field region with width l=3 within two building blocks. For convenience the structures are labeled with "symmetric" or "asymmetric" according to the symmetry of the corresponding vector potential.

In Figure 1 the "symmetric" structure is studied. The tunneling time is plot as a function of the electronic energy at several incident angles and under the applied biases $V_a = 0, 0.5, 1.0$. Here the incident angle is relative to the x direction [$\theta = \sin^{-1}(k_y/\sqrt{2E})$] and the bias is given in units of $\hbar\omega_c/e$. The left and right panels correspond to the case of $k_y \geqslant 0$ and $k_y \leqslant 0$, respectively. One remarkable fact is that for electrons traversing the considered structure with different incident angles, the distinction of the tunneling time can approach several orders of magnitude. Therefore, electrons incident at different angles will spend quite different time through the same structure, and are separated in time if they begin tunneling simultaneously. In the case of normal incidence ($\theta = 0$) and under zero bias, the tunneling time decays essentially with the incident energy. If instead of oblique crossing with $\theta > 0$, as shown in Figure 1(p1), the curve displays weak oscillations and has several kinks (local minima), which shift towards high-energy region with θ increasing. When electrons are incident at a negative θ, however, the kink appears only at large $|\theta|$, see Figure 1(n1). At each negative θ, when the incident energy is lower than some value the tunneling time is shorter than the counterpart of $\theta = 0$. Such a variation is in contrast to the case of positive θ where the tunneling time always prolongs significantly with θ increasing. Under a finite bias, the discrepancy of tunneling time is lessened for electrons with different negative incident angles. Whereas in the case of $\theta > 0$, the difference is still obvious. Moreover, one can observe the crossing between the curves for different positive incident angles [see Fig. 1(p3)], which is not seen in the absence of an applied bias. With the bias increasing, the tunneling time is drastically shortened and the kinks move towards the low-energy region.

All features described above reflect the structure of the effective potential to some extent. For the "symmetric" MB structure under zero bias, the corresponding profile of U_{eff} seen by electrons with $k_y \geqslant 0$ is a symmetric electric double-barrier structure and the middle region with $B = 0$ acts as a quantum well. The barriers go up monotonously as k_y increases. In general, a larger incident energy will shorten the tunneling time since it means a larger initial velocity. This is true in the case of normal incidence where the height of barriers is invariant with the incident energy, but is not suitable for the case of a certain positive angle. The reason is that for $\theta > 0$ the barriers are also rising with the energy increasing due to the augment of corresponding k_y (recalling the relation $k_y = \sqrt{2E}\sin\theta$). Usually, the higher the barriers are, the longer the Bohm tunneling time is. The interplay of these two factors leads to the appearance of kinks. For $k_y < 0$ the effective potential is multiple wells in which the transmission is through states above quantum wells [7]. So the tunneling time for a negative θ may be shorter than that of $\theta = 0$ in some energy region. With $|k_y|$ increasing, the effective potential exhibits complex variation and the wells become deeper. Instead of the obstacle effect of the barriers, the factor leading to the prolonging of the tunneling time is now the binding of wells on electrons. In the presence of an external electric field, the electrons are accelerated and the tunneling time is thus shortened significantly. In addition, the symmetry of the effective potential is greatly changed by the applied bias [24], which results in rich electric-field-dependent behaviors of the tunneling time.

Figure 2 shows the variation of tunneling time with the incident energy for electrons traversing the "asymmetric" structure at zero and several positive incident angles. In this case the effective potential behaves like an asymmetric electric double-barrier structure where the asymmetry is introduced by the height difference between two building blocks. The left panels correspond to the left-to-right direction of tunneling, while the right ones refer to the right-to-left tunneling which is equivalent to

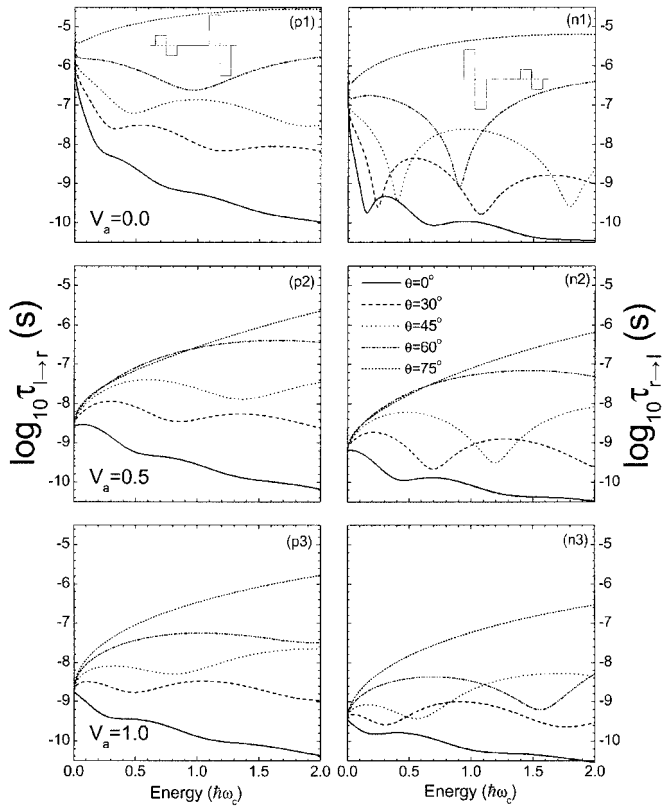

Fig. 2. The tunneling time for electrons traversing an "asymmetric" MB structure at zero and several positive incident angles under zero and two applied biases. The structure depicted in the inset of panel (p1) is composed of a block A (B_1=0.1 T and d_1= 1)and a block B (B_2=0.3 T and d_2= 1) separated by a zero magnetic-field region with width l=3. The left and right panels correspond to left-to-right and right-to-left tunneling direction, respectively. Note that the right-to-left tunneling is equivalent to the left-to-right tunneling through the structure depicted in the inset of panel (n1). V_a=0, 0.5, 1.0.

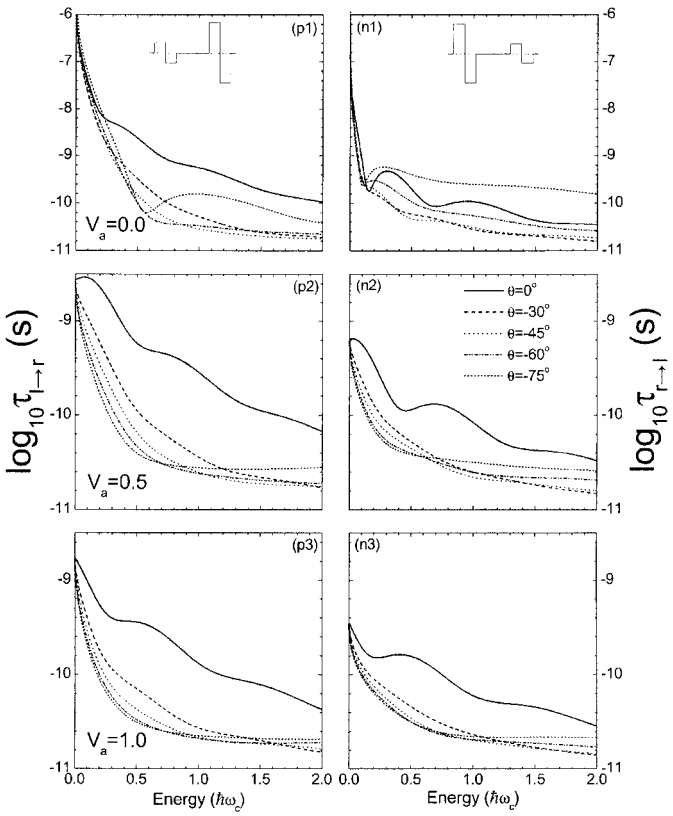

Fig. 3. The tunneling time for electrons traversing the structure as that examined in Figure 2 at zero and several negative incident angles under zero and two applied biases. The left and right panels correspond to left-to-right and right-to-left tunneling, respectively. V_a=0, 0.5, 1.0.

the left-to-right tunneling through the structure depicted in the inset of Figure 2(n1). One can see pronounced difference of the tunneling time between these two situations. Several features are summarized here. (1) The left-to-right tunneling time $\tau_{l\to r}$ is usually much greater than the corresponding $\tau_{r\to l}$. This fact can be understood from the definition of the Bohm tunneling time [$\tau = \int_0^L \mathrm{d}x\,|\Psi|^2 / k_R$ with $\Psi\,|_{x=L}$= 1, see Eq. (3)]. For the left-to-right tunneling through an asymmetric double-barrier structure, if the right barrier is higher, the module of the wave function decays more rapidly to the final value 1. Therefore, the probability of finding the particle in the tunneling structure is larger, which leads to longer tunneling time. (2) At zero bias, $\tau_{l\to r}$ oscillates weakly with the incident energy, which is very similar to that in the "symmetric" structure. The right-to-left tunneling time $\tau_{r\to l}$, however, displays strong oscillations and several sharp dips. In general, the tunneling time has relative minima at the value of incident energy where the transmission coefficient has relative maxima [20]. The reason is that at resonance the particle has maximal probability to appear within the tunneling region. With the bias increasing, the oscillation of $\tau_{r\to l}$ is suppressed and the dips become shallower. (3) For $\tau_{r\to l}$, even at zero bias there exists notable crossing between the curves for different incident angles. In the case of left-to-right tunneling, the crossing is not obvious and only occurs between large incident angles under some biases. This indicates that either with or without the influence of an applied bias, electrons with different positive incident angles during tunneling from the left to right will be more separated in the time scale than the right-to-left case.

As a complement of Figure 2, Figure 3 presents the case of $\theta \leqslant 0$. Comparing with the case in the "symmetric" structure, one can see that the tunneling time in the "asymmetric" structure exhibits apparent decaying with the incident energy. Note that with $|\theta|$ increasing, both $\tau_{l\to r}$ and $\tau_{r\to l}$ are usually shortened and greatly lower than the tunneling time of the normal incidence, which is opposite to the counterpart in the "symmetric" structure. The exception of the observation happens at large incident energy where the crossing phenomenon appears, or at large $|\theta|$ and under zero bias where the tunneling time may be greater than that of $\theta = 0$. At negative θ with large absolute value (for example $-75°$), there are one or several incident energies for which the

tunneling time has no difference between both directions. Accordingly, the geometric asymmetric structure becomes a symmetric one with respective to the tunneling time. For positive θ no such transition occurs and the structure is completely asymmetric regarding the tunneling time.

Finally, we would like to point out that although our consideration of the rectangular magnetic-barrier structures gives only a qualitative picture, nevertheless the time characteristics mentioned above should be present in the more realistic cases with barriers of smooth shape. Indeed these features do not depend on the actual shape of the magnetic-barrier but only on the presence of the barrier in the effective potential $U_{eff}(x, k_y, V_a)$. In addition, as we have stated, up to now how to define a physical time is still in controversy. Different definitions of the tunneling time reflect different aspects of electron dynamics, thus give rather different results even for a single electric barrier. Among them the Bohm tunneling time is shown to be in good agreement with some experiments (see Ref. [26]). Therefore, our work is expected to give meaningful results and can reflect one aspect of dynamical behaviors in the considered structure.

4 Conclusions

In summary, we present a feasible numerical method for tunneling time calculation in magnetic barrier structures based on the group velocity concept. The results reveal pronounced separation in time among the tunneling processes for electrons with different longitudinal wave vector. At a positive incident angle, the tunneling time differs significantly from that at a negative one with the same absolute value. The distinction embodies not only in the order of magnitude, but also in the variation with incident energy and with the bias. In the structure arranged with identical magnetic barriers and wells, an applied bias will reduce the degree of separation in time. For electrons tunneling through the structure composed of two different building blocks, the typical feature is that the tunneling time is related to the direction of the incoming electrons. The discrepancy for opposite directions in the time scale shows complex variation with the incident energy and depends strongly on the incident angles as well as the external electric field.

This work was supported by the National Natural Science Foundation of China (Grant No. 10004006) and by the National Key Project of Basic Research Development Plan (Grant No. G2000067107).

References

1. M.A. McCord, D.D. Awschalom, Appl. Phys. Lett. **57**, 2153 (1990)
2. C.L. Foden, M.L. Leadbeater, J.H. Burroughes, M. Pepper, J. Phys. Cond. Matt. **6**, L127 (1994)
3. M.L. Leadbeater, S.J. Allen, Jr., F. DeRosa, J.P. Harbison, T. Sands, R. Ramesh, L.T. Florez, V.G. Keramidas, J. Appl. Phys. **69**, 4689 (1991); K.M. Krishnan, Appl. Phys. Lett. **61**, 2365 (1992); W. Van Roy, E.L. Carpi, M. Van Hove, A. Van Esch, R. Bogaerts, J. DeBoeck, G. Borghs, J. Magn. Magn. Mater. **121**, 197 (1993); R. Yagi, Y. Iye, J. Phys. Soc. Jpn **62**, 1279 (1993)
4. A.K. Geim, Pis'ma Zh. Eksp. Teor. Fiz. **50**, 359 (1989) [JETP Lett. **50**, 389 (1990)]; S.J. Bending, K. von Klitzing, K. Ploog, Phys. Rev. Lett. **65**, 1060 (1990); A.K. Geim, I.V. Grigorieva, S.V. Dubonos, J.G.S. Lok, J.C. Maan, A.E. Filippov, F.M. Peeters, Nature (London) **390**, 259 (1997)
5. F.M. Peeters, P. Vasilopoulos, Phys. Rev. B **47**, 1466 (1993); H.A. Carmona, A.K. Geim, A. Nogaret, P.C. Main, T.J. Foster, M. Henini, Phys. Rev. Lett. **74**, 3009 (1995); P.D. Ye, D. Weiss, R.R. Gerhardts, M. Seegar, K. von Klitzing, K. Eberl, H. Nickel, Phys. Rev. Lett. **74**, 3013 (1995); S. Izawa, S. Katsumoto, A. Endo, Y. Iye, J. Phys. Soc. Jpn **64**, 706 (1995)
6. H.-S. Sim, K.H. Ahn, K.J. Chang, G. Ihm, N. Kim, S.J. Lee, Phys. Rev. Lett. **80**, 1501 (1998); J. Reijniers, F.M. Peeters, A. Matulis, Physica (Amsterdam) E **6**, 759 (2000); A. Nogaret, S.J. Bending, M. Henini, Phys. Rev. Lett. **84**, 2231 (2000); H.-S. Sim, G. Ihm, N. Kim, K.J. Chang, Phys. Rev. Lett. **87**, 146601 (2001); J. Reijniers, F.M. Peeters, J. Phys. Cond. Matt. **12**, 9771 (2000); S. Badalyan, F.M. Peeters, Phys. Rev. B **64**, 155303 (2001)
7. M. Matulis, F.M. Peeters, P. Vasilopoulos, Phys. Rev. Lett. **72**, 1518 (1994)
8. Y. Guo, B.L. Gu, W.H. Duan, Y. Zhang, Phys. Rev. B **55**, 9314 (1997); Y. Guo, B.L. Gu, Z.Q. Li, J.Z. Yu, Y. Kawazoe, J. Appl. Phys. **83**, 4545 (1998); Y. Guo, B.L. Gu, Z.Q. Li, J.L. Zhu, Y. Kawazoe, J. Phys. Cond. Matt. **10**, 1549 (1998)
9. M. Johnson, B.R. Bennett, M.J. Yang, M.M. Miller, B.V. Shanabrook, Appl. Phys. Lett. **71**, 974 (1997); A.K. Geim, S.V. Dubonos, J.G.S. Lok, I.V. Grigorieva, J.C. Maan, L.T. Hansen, P.E. Lindelof, Appl. Phys. Lett. **71**, 2379 (1997); V. Kubrak, F. Rahman, B.L. Gallagher, P.C. Main, M. Henini, C.H. Marrows, M.A. Howson, Appl. Phys. Lett. **74**, 2507 (1999)
10. Z.Y. Zeng, L.D. Zhang, X.H. Yan, J.Q. You, Phys. Rev. B **60**, 1515 (1999)
11. Y. Guo, H. Wang, B.L. Gu, Y. Kawazoe, Phys. Rev. B **61**, 1728 (2000); Y. Guo, B.L. Gu, Z. Zeng, J.Z. Yu, Y. Kawazoe, Phys. Rev. B **62**, 2635 (2000)
12. I.S. Ibrahim, F.M. Peeters, Phys. Rev. B **52**, 17 321 (1995)
13. D. Bohm, *Quantum Theory* (Englewood Cliffs, NJ: Prentice Hall, 1951), pp. 257–261; E.P. Wigner, Phys. Rev. **98**, 145 (1955)
14. F.T. Smith, Phys. Rev. **118**, 349 (1955)
15. A.I. Baź, Sov. J. Nucl. Phys. **4**, 182 (1967); V.F. Rybachenko, *ibid.* **5**, 635 (1967); M. Buttiker, Phys. Rev. B **27**, 6178 (1983); M. Buttiker, R. Landauer, Phys. Rev. Lett. **49**, 1739 (1982)
16. C. Leavens, Solid. State. Commun. **74**, 923 (1990); A.P. Jauho, M. Jonson, *ibid.* **6**, 303 (1989)
17. For a review see: R. Landauer, T. Martin, Rev. Mod. Phys. **66,** 217 (1994); S. Collins, D. Lowe, J.R. Barker, J. Phys. C **20**, 6213 (1987)
18. A.M. Elabsy, Physica B **292**, 233 (2000)
19. O. Voskoboynikov, S.S. Liu, C.P. Lee, Solid State Commun. **115**, 477 (2000)

20. D. Dragoman, M. Dragoman, IEEE J. Quantum Electronics **32**, 1150 (1996)
21. D. Dragoman, IEEE J. Quantum Electronics **35**, 1887 (1999)
22. A.M. Steinberg, P.G. Kwiat, R.Y. Chiao, Phys. Rev. Lett. **71**, 708 (1993); Ch. Spielmann, R. Szipöcs, A. Stingl, F. Krausz, Phys. Rev. Lett. **73**, 2308 (1994)
23. P. Pereyra, Phys. Rev. Lett. **84**, 1772 (2000)
24. Y. Guo, B. Wang, B.L. Gu, Y. Kawazoe, Eur. Phys. J. B **23**, 509 (2001)
25. A.F.M. Anwar, A.N. Khondker, M.R. Khan, J. Appl. Phys. **65**, 2761 (1989)
26. P. Thanikasalam, R. Venkatasubramanian, M. Cahay, IEEE J. Quantum Electronics **29**, 2451 (1993)
27. C. Bracher, M. Kleber, M. Riza, Phys. Rev. A **60**, 1864 (1999)
28. V.M. de Aquino, V.C. Aguilera-Navarro, M. Goto, H. Iwamoto, Phys. Rev. A **58**, 4359 (1998)
29. N. Yamada, Phys. Rev. Lett. **83**, 3350 (1999)
30. G. Papp, F.M. Peeters, Appl. Phys. Lett. **79**, 3198 (2001)
31. H.P. William, T.V. William, A.T. Saul, P.F. Brian, *Numerical recipes in C: The Art of Scientific Computing* (Cambridge University Press, New York, 1986), Chap. 18